Published in final edited form as:
Cancer Gene Ther. 2009 March ; 16(3): 217–226. doi:10.1038/cgt.2008.79.

Imaging of cationic multifunctional liposome-mediated delivery of COX-2 siRNA

M Mikhaylova[1], **I Stasinopoulos**[1], **Y Kato**[1], **D Artemov**[1,2], and **ZM Bhujwalla**[1,2]

[1]JHU ICMIC Program, The Russell H Morgan Department of Radiology and Radiological Science, The Johns Hopkins University School of Medicine, Baltimore, MD, USA

[2]Sidney Kimmel Comprehensive Cancer Center, The Johns Hopkins University, School of Medicine, Baltimore, MD, USA

Abstract

Liposomes are a useful means of delivering molecular targeting agents such as small interfering RNA (siRNA) to downregulate specific pathways important in cancer growth and progression. The ability to non-invasively image these carriers is important to ascertain their delivery within the tumor. As cyclooxygenase-2 (COX-2) is an important therapeutic target in cancer, we investigated loading COX-2-specific siRNA into cationic liposomes containing MR contrast agents for imaging delivery in cancer cells and tumors. COX-2 and GAPDH siRNA, as well as Magnevist or Feridex, were loaded directly into the liposomes. These lipoplexes were used for cell transfection of the poorly differentiated and highly metastatic breast cancer cell line MDA-MB-231. PEGylated liposomes loaded with Feridex and fluorescently labeled COX-2 siRNA were used for *in vivo* delivery of lipoplexes in MDA-MB-231 breast cancer xenografts in female SCID mice. Transient transfection assays demonstrated potent and specific downregulation of the COX-2 protein in cells in culture. Tail vein injections of PEGylated COX-2 lipoplexes resulted in intratumoral delivery of siRNA. Biodistribution studies showed significant localization in the lung, liver and kidney at 24 h. These data demonstrate the feasibility of liposomal-mediated delivery of COX-2-specific siRNA to downregulate COX-2 in cancer cells, and multi-modality imaging of the delivery of specific siRNA in tumors.

Keywords

siRNA; cyclooxygenase-2; breast cancer; multicomponent cationic liposome; MRI; optical imaging

Introduction

The cyclooxygenase (COX) pathway is the target of several clinical trials for diseases with high inflammatory components such as cancer. COX-2 is a cytoplasmic enzyme responsible for the conversion of arachidonic acid to active lipid mediators, the expression of which is induced by pro-inflammatory cytokines such as IL-1β. COX-2 is upregulated in different cancers such as colon,[1] prostate[2] and breast.[3] We have demonstrated earlier that silencing

Correspondence: Dr ZM Bhujwalla, The Russell H Morgan Department of Radiology and Radiological Science, The Johns Hopkins University School of Medicine, Traylor Building, Room 208C, 720 Rutland Avenue, Baltimore, MD 21205, USA. zaver@mri.jhu.edu.

Supplementary Information accompanies the paper on Cancer Gene Therapy website (http://www.nature.com/cgt)

COX-2 using a COX-2-specific short hairpin RNA molecule stably expressed in the poorly differentiated and highly metastatic breast cancer cell line MDA-MB-231 delayed tumor formation and inhibited extrapulmonary metastasis in an experimental model of metastasis.[4] The ability to effectively deliver COX-2 siRNA to tumors would provide a means to downregulate the COX-2 pathway as a novel therapeutic option.

Several vehicles for systemic delivery of small interfering RNA (siRNA) delivery such as cationic liposomes are currently being evaluated. Cationic liposomes have been used earlier as an alternative to viral delivery of nucleic acids, particularly for anticancer therapy.[5-8] Successful gene silencing has been achieved using commercially available liposome-based transfection reagents such as lipofectamine, oligofectamine or synthetically prepared liposomes[9,10] in cultured cells. Although the efficient delivery of siRNA-liposome complexes (lipoplexes) *in vivo* is limited by factors such as toxicity, enzymatic degradation, target specificity and poor vascular delivery,[11] several studies have described successful downregulation of target molecules using liposome-mediated delivery. The advantage of using liposomes as compared to other delivery systems is that they consist of sealed bilayer membranes made of largely naturally occurring lipids that are similar to biological membranes. Liposomes can fuse with cell membranes[12] so that the aqueous compartment becomes contiguous with the cytosol of the cell, delivering encapsulated material. DOTAP (1,2-dioleoyl-3-trimethylammonium-propane) liposomes have been used earlier to systemically deliver siRNA directed against TNF-α;[13] intraperitoneal injections of anti-TNF-α siRNA inhibited lipopolysaccharide-induced TNF-α gene expression.[14] Cationic DOTAP/DOPE (DOPE: 1,2-dioleoyl-*sn*-glycero-3-phosphoethanolamine) liposomes decorated with anti-transferrin receptor single-chain antibody fragment were used for targeted delivery of siRNA to primary (PC-3/Capan-1) and metastatic (MDA435/LCC6) tumor models.[15] Improved transfection efficiency was achieved using a pH-sensitive histidine-lysine peptide complexed to the liposomes for delivery of a modified HER-2-specific siRNA molecule.[16] Chemically modified 'siHybrid' molecules have also been used against MDA-MB-435 human cancer xenografts in mice and showed greater inhibition of HER-2 expression and induction of apoptosis as compared to unmodified siRNA.[17] Delivery of galactosylated lipoplexes to liver parenchymal cells resulted in 80% inhibition of the endogenous Ubc13 gene expression.[18] LIC-101 cationic liposomes were used to deliver bcl-2-specific siRNA to tumor cells in the mouse liver and showed inhibition of tumor cell growth in a prostate cancer model after intravenous administration of the complex.[19] Although several studies have demonstrated the efficient delivery of siRNA *in vivo* using fluorescence[16,18,19] and bioluminescence imaging,[20] relatively few studies have used non-invasive magnetic resonance imaging (MRI) to monitor siRNA delivery.[21]

In this study, we investigated the possibility of directly loading COX-2-specific siRNA into DOTAP/DOPE and DOTAP/DOPE/DOPE-PEG2000 (PEG2000: polyethylene glycol, MW 2000 Da) cationic liposomes. Multi-functional liposomes were prepared by lipid hydration and loaded with fluorescently labeled siRNA during the hydration step. We tested iron (Fe)- and gadolinium (Gd)-based contrast agents incorporated into the liposomes for MRI detection of delivery, and observed that iron, but not Gd-based contrast agents, could be incorporated to lipoplexes without loss of COX-2 siRNA-mediated target specificity. To prevent recognition by macrophages and prolong circulation of lipoplexes *in vivo*, cationic liposomes were decorated with PEG. Our results demonstrate successful intratumoral delivery as detected by imaging of DY647-labeled COX-2-specific siRNA (optical imaging) delivered by PEGylated and Feridex-loaded lipoplexes (MRI) in the MDA-MB-231 human breast cancer xenograft model.

Materials and methods

Cell culture

MDA-MB-231 cells were originally derived from the pleural effusion of a breast cancer patient[22] and grown as a monolayer in RPMI 1640 (Sigma-Aldrich, St Louis, MO) medium supplemented with 8.25% fetal bovine serum (FBS). Cells were incubated at 37 °C in a humidified incubator with 5% of CO_2. Medium was changed every 2–3 days.

Cationic lipids and contrast agents

Cationic lipids DOTAP, DOPE, DOPE-PEG2000 and DOPE-RhodB were purchased from Avanti Polar Lipids (Alabaster, AL). Gadolinium (Gd-BOA) was obtained from Gateway Chemical Technology Inc. (St Louis, MO). Magnevist (Gd-DTPA) and Feridex (dextran-coated iron oxide nanoparticles) were obtained from Bayer Health-Care Pharmaceuticals (Advanced Magnetics Inc., Cambridge, MA). A commercially available transfection reagent, Lipofectamine 2000 (L2000), was purchased from Invitrogen (Carlsbad, CA).

siRNA

siRNA was purchased from Dharmacon Research (Lafayette, CO) with the following sequences for COX-2 siRNA—sense: 5′-CAUUCCCUUCCUUCGAAAUdT dT-3′ and antisense: 5′-AUUUCGAAGGAAGGGAA UGdTdT-3′ and for control siRNA against GAPDH sense: 5′-UGGUUUACAUGUUCCAAUAUU-3′ and antisense: 5′-PUAUUGGAACAUGUAAACCAUU-3′.

COX-2 siRNA was additionally labeled with fluorescein 5(6)-isothiocyanate (FITC) for cell studies and with DY647 for *in vivo* studies (Dharmacon Research).

Preparation, loading with siRNA and characterization of liposomes

For cell studies, cationic liposomes DOTAP/DOPE (3:1 molar ratio) abbreviated as DD and DOTAP/DOPE/DOPE-PEG2000 (3:0.95:0.05 molar ratio) abbreviated as DDP were prepared using the lipid hydration method. Briefly, lipids (total 3 mmol, 1 mg ml^{-1} of total lipids) were dissolved in chloroform and a small amount (0.2 mol %) of DOPE-rhodamine B was added to confirm internalization and localization in cells using fluorescence microscopy. The solvent was removed by evaporation using argon flow and residual chloroform was removed overnight using a rotary evaporator. siRNA against COX-2 and GAPDH were prepared from a stock solution (100 mM) in reduced-serum medium (OPTIMEM; Invitrogen). The lipid film was then hydrated with OPTIMEM containing siRNA molecules such that the final liposome concentration for cell transfections was approximately 40 μgml^{-1} and the final concentration of siRNA was approximately 40 nM. After hydration for 10–15 min, the suspension was slowly vortexed and complexes allowed to form for an additional 20 min. The DD and DDP liposomes were also loaded with three different contrast agents, Gd-BOA (DDGd and DDPGd), or Magnevist (DDM and Gd-DTPA, 5 mM) or Feridex (DDFe and DDPFe 110 μgml^{-1}). Gd-BOA was incorporated within lipid bilayers in place of 50 mol % of the DOTAP during the formation of liposomes, so that the final concentration of contrast agent was 37.5 mol % in the final liposome formulation. Magnevist or Feridex were added during the hydration step without changes in the lipid ratio.

The excess of Magnevist was removed using a Millipore microcon filter spin column (YM 100; Millipore Corporation, Bedford, MA). The charge ratio of nucleic acid backbone phosphates to cationic lipid/Magnevist was 0.1:0.004:1.

To analyze the incorporation of Feridex in the liposomes, we purified DDPFe lipoplex using size-exclusion chromatography with Sepharose CL-2B beads (SigmaAldrich). Several fractions were collected and analyzed for size distribution. The fractions that had values of size distribution comparable to the size of liposomes before purification were additionally characterized with respect to their T_2 values and lipid concentration.[23] We found that T_2 values did not significantly change after the purification step (Supplementary Table 1), indicating undetectable levels of free Feridex.

Additionally, we separated unincorporated DY-647-labeled siRNA using a Microcon YM-100 size-exclusion spin column. No fluorescence was detected in the eluate using a UV–VIS spectrophotometer (Beckman Coulter, DU, Fullerton, CA). In contrast, significant fluorescence was detected in the lipoplexes retained in the excluded top part of the column following centrifugation at 500 *g* for 12 min (data not shown). We therefore concluded that most of the siRNAs was incorporated into the liposomes. DY-647-labeled siRNA was used to avoid the background absorbance observed due to the presence of liposomes between 230 and 550 nm. Using a similar method, we estimated that the loss of the siRNA during the extrusion step is about 5%.

The concentration of Gd^{3+} and iron ions in the final lipolex suspensions were determined by inductively coupled plasma mass spectrometry (ICP-MS) (Perkin Elmer/Sciex Elan DRC II, Concord, ON, Canada).

T_1 and T_2 relaxation times were measured at a 9.4 T MR Spectrometer (Bruker BioSpin GmBH, BioSpec, Rheinstetten, Germany). T_1 relaxation times of DDGd, DDPGd and DDM lipoplexes were measured with a saturation recovery sequence. In these experiments, the repetition time (TR) was 8 s, the echo time (TE) was 1.142 ms, the field of view was 3.2 cm, matrix size was 128 × 64, the number of averages (NA) was 4 and the slice thickness was 1 mm. The saturation recovery times were 10, 20, 50, 100, 200, 400, 800, 1000, 2000 and 4000 ms.

The T_2 relaxation times of DDFe and DDPFe lipoplexes were measured with a T_2-weighted MSME sequence. Acquisitions with a TR of 500 ms, and TE of 8, 16, 24, 32, 40 and 48 ms, number of averages of 4, 1 slice and slice thickness of 1 mm were used. The images were reconstructed using custom-written software in the Interactive Data Language (IDL) programming environment. The final analysis of T_1 and T_2 values was performed with ImageJ (National Institute of Health, Bethesda, MD) (Supplementary Table 1).

For *in vivo* experiments, 200 μl of DDP liposome/siRNA complex (10 mg ml^{-1} and 150 μl of 100 μM) with a calculated charge ratio of nucleic acid backbone phosphates to cationic lipid 1:3 was passed through a 100 nm pore size polycarbonate membrane using a sterile extruder (Avestin Inc., Canada), washed earlier with nuclease-free sterile water to prevent degradation of siRNA during the extrusion step.

The hydrodynamic diameters of lipoplexes used for the *in vivo* experiments were measured in OPTIMEM and their ζ potential in 10 mM of NaCl at 25 °C in two independent experiments using a Malvern Zetasizer (Malvern Instruments Inc., Southborough, MA). Each measurement was repeated at least three times.

MTT cell viability assay

MDA-MB-231 cells (2×10^3) were seeded in 96-well plates and allowed to recover from trypsinization for 24 h. Liposomes alone and COX-2 and GAPDH lipoplexes were added and plates were returned to a tissue culture incubator for 4 h. The medium was then replaced with RPMI 1640 supplemented with 8.25% FBS without phenol red and cells were cultured

for an additional 20 h. After incubation, 10 μl of 3-(4,5-dimethylthiazol-2-yl)-2,5-diphenyltetrazolium bromide (MTT) dye solution (ATCC Bioproducts, Manassas, VA) was added into each well and cells were incubated for an additional 4 h. In total, 100 μl of detergent reagent was then added to each well and plates were incubated overnight in the dark at room temperature. The absorbance was read on a Victor plate reader at 550 and 630 nm (Perkin Elmer Life and Analytical Sciences Inc., Waltham, MA). Viability was calculated using the following equation: $(A_{550}–A_{630})$ cells with liposomes or lipoplexes × 100%/$(A_{550}–A_{630})$ cells without liposomes.

Cell transfections

MDA-MB-231 cells were seeded at 60–70% confluence and transfected with 200 μl of lipoplexes (40 $\mu g ml^{-1}$ of total lipids and 40 nM of siRNA) in RPMI 1640 medium supplemented with 8.25% FBS and incubated for 4, 8 and 24 h as indicated. The medium was then replaced and cells were returned to the incubator for an additional 20, 16 and 0 h, respectively. To monitor transfection efficiency, Lipofectamine 2000 (Invitrogen) was used as a positive control according to the manufacturer's protocol.

Western blot analyses

To determine COX-2 and GAPDH protein expression levels, MDA-MB-231 cells (1.7×10^6) were seeded in 100 mm Petri dishes and transfected with lipoplexes for 24 h. Cells were washed once with 1 × PBS, harvested, centrifuged and resuspended in mammalian protein extraction reagent, M-PER (Pierce, Rockford, IL) solution with protease inhibitor cocktail (1:750; Sigma-Aldrich). The total protein amount was determined using the D_C protein assay (Bio-Rad, Hercules, CA). Immuno-blotting was performed following standard protocols. The Immobilon transfer membrane (Millipore Corporation) was incubated overnight at 4 °C with COX-2 polyclonal antibody (1:1000; Cayman Chemical, Ann Arbor, MI) or for 1 h with GAPDH polyclonal antibody (Santa Cruz Biotechnology, Santa Cruz, CA) or actin monoclonal antibody (1:50 000; Jackson Immunoresearch Laboratories Inc., West Grove, PA) in 5% skimmed milk. Horseradish peroxidase-conjugated secondary anti-rabbit, anti-goat and anti-mouse antibodies (1:2000; Jackson Immunoresearch Laboratories Inc.) were added and proteins were visualized using WestPico Chemiluminescence detection reagent (Pierce).

Optical imaging

For the cell experiments, MDA-MB-231 cells (5×10^4) were seeded in 750 μl of RPMI 1640 medium supplemented with 8.25% FBS in four chamber slides (Nalge Nunc International, Rochester, NY). Cells were transfected as described above using a scaled down amount of lipoplexes. After 24 h, cells were washed three times with 1 × PBS, fixed with 3% of paraformaldehyde and imaged using a Nikon ECLIPSE-TS100 fluorescence microscope (Nikon Instrument Inc., Melville, NY). Images were digitized using a Nikon Coolpix 5000 digital camera (Nikon Corporation, Tokyo, Japan).

In vivo *delivery and imaging*

All *in vivo* studies were performed in compliance with institutional guidelines established by the Institutional Animal Care and Use Committee of Johns Hopkins University. A total of 14, 5- to 6-week old female SCID mice were inoculated subcutaneously in the mammary fat pad with 2×10^6 MDA-MB-231 cells suspended in 50 μl of Hanks balanced salt solution. When tumor sizes reached ~200 mm^3, 250–280 μl of DDP-DY647-labeled COX-2 lipoplexes were injected intravenously (i.v.) and mice were imaged with a Xenogen IVIS 200 optical imaging device (data not shown). DY647-labeled COX-2 siRNA without liposomes were also injected i.v. and used as a control. Animals were killed at 0.5, 3, 8 and

24 h time points and tumor, liver, kidney, spleen, lungs and stomach were imaged as separate organs. For biodistribution studies, mice (n = 3) were injected with lipoplexes for 24 h and 1-mm-thick slices of organs and tumor were imaged using the Xenogen IVIS system. Instrument settings were normalized to identical exposures for image processing and quantification. For fluorescence studies, organs and tumors were frozen in liquid N_2, embedded in OCT (Optimal Cutting Temperature) compound medium for frozen tissue specimens; (Sakura Finetek, USA Inc., Torrance, CA, USA), and stored at −80 °C until further use. Each organ was cut in 10-μm-thick sections, fixed with 3% of paraformaldehyde and examined by fluorescence microscopy using a Nikon ECLIPSE-TS100 microscope (Nikon Instrument Inc.). Nuclei were stained with DAPI (4,6-diamidino-2-phenylindole) (ProLong Gold antifade reagent; Invitrogen, Molecular Probes, Eugene, OR).

Additionally, DDP-COX-2 lipoplexes were loaded with Feridex to monitor the delivery of siRNA using MRI. In this set of experiments, a total of five tumor-bearing female SCID mice were injected i.v. with DDPFe-COX-2 lipoplexes. Tumors were imaged at 3 and 24 h post-injection on a Bruker 9.4 T horizontal bore (Bruker BioSpin GmBH, Rheinstetten, Germany) spectrometer using a T_2-weighted 3D RARE (rapid acquisition with rapid enhancement, TR = 500 ms, TE = 30, 50 and 100 ms, field of view 16 × 16 × 8, matrix size 128 × 64 × 32, zerofilled to 128 × 128 × 64, NOA = 2) sequence. The resulting spatial resolution was 0.125 mm × 0.125 mm × 0.125 mm. Images were processed using custom tools developed in IDL (ITT Visual Information Solutions, Boulder, CO). T_2-weighted 3D RARE images (TE = 50 ms) at 0, 3 and 24 h were aligned by affine registration using Amira (Visage Imaging, Carlsbad, CA). Subsequently, histogram intensities of each image at 3 and 24 h post-injection were normalized to the histogram intensities from pre-contrast images. Representative slices of the tumor at each time point were identified, and the histograms for a region of interest computed using ImageJ. T_2-weighted 3D RARE images (TE = 30, 50 and 100 ms) were also processed using IDL to obtain quantitative T_2 maps. T_2 maps at 0, 3 and 24 h post-injection were co-registered and analyzed in the same manner as described above. After MRI experiment, animals were killed and the tumors were frozen in OCT for immunohistochemistry. To confirm the presence of Feridex within tumors, 10-μm frozen sections were stained with anti-dextran FITC antibody (StemCell Technologies Inc., Vancouver, BC, Canada) and nuclei were stained with DAPI. Images were taken using a Nikon ECLIPSE-TS100 microscope.

Liver toxicity test

Alanine aminotransferase (ALT) and aspartate aminotransferase (AST) were purchased from Pointe Scientific Inc. (Canton, MI). Levels of ALT and AST in the serum were checked at 24 h post-intravenous injection from mice injected with DDPFe-COX-2 lipoplexes (n = 3) and from uninjected mice (n = 3).

Statistical analysis

MRI data were analyzed and presented as mean±s.e.m. P-values were determined by an unpaired Student's t-test. P <0.05 was considered significant.

Results

Lipoplex preparation and characterization

Cationic liposomes DD, DDFe, DDGd, DDM, DDP, DDPFe and DDPGd were prepared by lipid hydration from the corresponding lipids. The contrast agents Magnevist or Feridex were loaded directly during lipid hydration with OPTIMEM and Gd-BOA was incorporated within lipid bilayers during the formation of DDGd and DDPGd liposomes. For *in vivo* experiments, lipoplexes were extruded using a 100 nm polycarbonate membrane. Physical

characteristics of extruded lipoplexes are shown in Table 1. The hydrodynamic diameter of COX-2-bearing lipoplexes was in the range of 260–310 nm. The presence of PEG on the surface of liposomes resulted in steric stabilization of lipoplexes except for DDPFe formulation (Table 1) reducing their diameter to ~100 nm. Incorporation of Gd-BOA or Feridex contrast agents in lipoplexes resulted in a modest decrease of their positive surface charge; incorporation of Magnevist did not affect the surface charge of the lipoplexes. Incorporation of contrast agents significantly increased the polydispersity index (PDI) values of DD lipoplexes. Addition of PEG to lipoplexes resulted in steric stabilization with the exception of DDPFe the diameter of which was not affected. Addition of PEG to DDGd lipoplexes reduced their PDI value. DDP, DDPFe and DDM PDI values were not significantly altered on PEGylation. The ζ potential values of lipoplexes were decreased following PEGylation, but remained positive. Incorporation of siRNA into DDP liposomes increased the size and broadened the size distribution as compared to DDP liposomes alone (Figure 1, middle and top panels). Extrusion of DDP-COX-2 siRNA lipoplexes reduced the size of the lipoplexes (Figure 1, middle and lower panels).

DD and DDP lipoplexes are internalized in MDA-MB-231 cells within 0.5 h

To examine the internalization of liposomes in cell culture, rhodamine B-labeled liposomes alone or FITC-labeled COX-2 siRNA lipoplexes were incubated with MDA-MB-231 cells. Uptake of DD and DDP liposomes and DD- and DDP-FITC-COX-2 lipoplexes was analyzed by fluorescence microscopy. A majority of the liposomes were internalized within the first 0.5 h (Figure 2a, left). siRNA-loaded DD and DDP lipoplexes were also readily internalized in MDA-MB-231 cells (Figure 2a). Naked siRNA molecules were not internalized in the absence of liposome vehicles after 4, 8 or 24 h (data not shown).

PEGylated lipoplexes have low toxicity in cells

The toxicity of liposomes and lipoplexes was assessed using the MTT cell viability assay (Figure 2b). Lipofectamine 2000 (L2000) and cells without any liposomes or lipoplexes were used as controls. No significant changes in MDA-MB-231 cell viability were observed following 24 h of incubation with liposomes alone. DD-based lipoplexes resulted in a significant reduction of cell viability, but this was not evident when lipoplexes were PEGylated (Figure 2b).

DD and DDP lipoplexes specifically downregulate COX-2

Initially, we loaded DD liposomes with different concentrations of COX-2 siRNA (4, 8 and 16 nM) and transiently transfected MDA-MB-231 cells with DD lipoplexes (Figure 3a, left panel). L2000 (lane L) was used as a positive control to standardize transfection efficiency. Dose-dependent downregulation of COX-2 protein following DDCOX-2 lipoplex transfection for 4 h was observed (Figure 3a, left). To demonstrate the sequence-specificity of the downregulation of protein expression by lipoplexes, GAPDH- and COX-2-specific siRNA molecules were used. Incorporation of Gd-BOA contrast agent into the DD lipoplexes resulted in the downregulation of COX-2 protein expression in MDA-MB-231 cells (Figure 3a, right) irrespective of the siRNA sequence. To examine the effect of PEGylation on the potency and specificity of lipoplexes, we performed transient transfection assays using DDP liposomes. The presence of PEG in the main formulation of DD lipoplexes did not affect the specificity or the potency of the lipoplexes in downregulating the expression of COX-2 or GAPDH (Figure 3a, right).

Gd-based contrast agents affect lipoplexes specificity

To determine whether extended incubation of DDP, DDGd and DDPGd lipoplexes would influence siRNA-mediated silencing of protein expression, MDA-MB-231 cells were

transfected for 4, 8 and 24 h. Incubation of DDP lipoplexes for extended periods demonstrated siRNA-dependent, sequence-specific downregulation of COX-2 and GAPDH protein expression. In contrast, Gd-BOA incorporation into DD and DDP lipoplexes resulted in nonspecific downregulation of protein expression following 4, 8 and 24 h of incubation with cells (Figures 3a and b). To investigate whether other commercially available contrast agents affected the potency and specificity of lipoplexes, we examined the effect of Magnevist and Feridex incorporation into the aqueous compartment of DD liposomes and transfected the lipoplexes for 4 h. Among the three contrast agents, only DDFe lipoplexes showed specific downregulation of COX-2 (Figure 3c) protein levels. Similar to the effects observed with DDGd, transfection with Magnevist-containing lipoplexes (DDM) resulted in a modest nonspecific downregulation of protein expression (Figure 3c).

DDP-COX-2 lipoplexes are localized in the tumor within 0.5 h post injection

To investigate the biodistribution of lipoplexes, we injected tumor-bearing female SCID mice with DDPCOX-2 lipoplexes and examined their localization using fluorescence microscopy 0.5, 3, 8 and 24 h following tail vein injection. DY647-labeled COX-2 siRNA was localized in the tumor as early as 0.5 h post-injection (Figure 4a) and continued to be present intratumorally 3, 8 and 24 h post-injection (Figures 4b–d). Intratumoral localization of DDP-delivered COX-2 siRNA was verified by overlaying the fluorescence with the corresponding phase-contrast image (left column) as well as by counter-staining the tumor sections with DAPI for nuclei (middle column). DY647-labeled siRNA was localized in the cytoplasm of tumor cells (middle and right columns). DY647-labeled COX-2 siRNA, without liposomes, predominantly accumulated in the bladder 0.5 h post-injection (data not shown).

Because we observed nonspecific downregulation of COX-2 siRNA in cells using DDGd, DDPGd and DDM lipoplexes in the presence of Gd^{3+} ions, but more specific downregulation of COX-2 in the presence of Fe (Feridex), using DDFe liposomes, we next examined the delivery of COX-2 siRNA using PEGylated DD liposomes loaded with Feridex. Representative T_2-weighted images of a tumor are shown in Figure 5a. These T_2-weighted images revealed changes in the contrast enhancement at 3 h as compared to the pre-contrast images. The decrease of signal intensity became even more prominent at 24 h (Supplementary Figures 1–3). On the histograms computed from T_2 maps (Figure 5b), a shift to lower T_2 values at 3 and 24 h is clearly seen, which indicates the presence of DDPFe-COX lipoplexes in the tumor. These data are in good agreement with data obtained with optical imaging. Analysis of the intensity of T_2 maps, quantified using ImageJ, is shown in Figure 5c. These data demonstrate that at 3 and 24 h post-injection of lipoplexes there o is a significant reduction of T_2 values ($n = 5$, $^*P < 0.004$ and $^{**}P = 0.02$).

Following the MRI experiments, animals were killed and frozen tumor sections were stained with anti-dextran antibody to confirm the presence of Feridex. A representative fluorescence microscopy image demonstrating the presence of Feridex in the tumor is shown in Supplementary Figure 2.

High fraction of undecorated DDP-COX-2 lipoplexes are localized primarily in the lungs

To investigate the localization of DDP-COX-2 lipoplexes, 10-μm sections of lungs, liver and kidney were obtained and analyzed by fluorescence microscopy. A strong fluorescent signal from COX-2 siRNA was observed in the lung and liver of injected animals as early as 0.5 h post-injection and this signal remains high at 3 h. In contrast, the fluorescent intensity in the kidney was lower at 0.5 h than at 3 h post-injection (Figures 6a and b). The localization of COX-2 siRNA at 8 h was more pronounced in the lungs and kidneys, whereas the

fluorescent intensity in liver diminished (Figure 6c). At 24 h post-injection, the overall amount of fluorescence was reduced (Figure 6d).

To quantify the biodistribution of fluorescent signal from DY647-labeled COX-2 siRNA lipoplexes, the fluorescence intensity of 1 mm organ and tumor sections obtained 24 h post-injection was digitized and measured using a Xenogen IVIS 200 (Figure 7). The highest fluorescence intensity was observed in lungs, kidney, stomach and liver. Tumor and spleen fluorescence was also detected, whereas no fluorescence could be detected in the heart or muscle.

To evaluate the effect of DDPFe-COX-2 lipoplexes on liver toxicity, we monitored the levels of AST and ALT in the serum from treated and control mice as elevated levels of AST and ALT reflect liver toxicity.[24] In this assay, DDPFe-COX-2 lipoplexes were injected every 24 h for 4 days and serum was collected on the fifth day, at 96 h post-injection. No significant differences were observed in AST ($P = 0.99$) and ALT ($P = 0.61$) levels between treated and control mice (Supplementary Figure 3).

Discussion

Inflammation is currently considered a major contributor to tumor progression and metastasis.[1-4] COX-2 function is targeted in many active clinical trials using COX-2-selective pharmacological inhibitors. The COX-2-independent functions of these inhibitors[25] have increased the demand for more potent and specific COX-2 inhibitors. Using a COX-2-specific shRNA, we demonstrated earlier that poorly differentiated metastatic breast cancer cells are dependent on the expression of COX-2 for tumor onset and extrapulmonary metastasis,[4] making COX-2 an attractive target in cancer. Here, we have characterized the efficacy of COX-2 downregulation in cells and detected the *in vivo* delivery of cationic liposomes directly loaded with COX-2 siRNA using optical and MR imaging.

Efficient non-viral delivery of siRNA requires stable formulation and targeting of lipoplexes to the growing tumors as well as specificity and functionality of the delivered siRNA cargo. Several recent reports have demonstrated the efficacy of DOTAP/DOPE cationic liposomes in delivering antisense oligonucleotides and siRNA to targeted tumors.[7,15,17]

In our study, lipoplexes were formed by mixing positively charged cationic liposomes with negatively charged siRNA in reduced serum medium. PEG was included in the lipoplex formulation to increase their circulation time following i.v. injection and to reduce the toxicity of the lipoplexes. The presence of PEG may affect the capacity of liposomes to carry siRNA molecules or decrease the efficiency of intracellular delivery. We therefore sought to improve the transfection efficiency of liposomes by mixing COX-2 siRNA with DDP lipids during the hydration step before the liposomes formed using pre-made PEGylated lipids. Earlier, PEGylated liposomes used to deliver antisense oligonucleotides or siRNA have been formed by attaching PEG moieties after the formation of the lipoplexes.[26] Santel *et al*.[27] recently demonstrated downregulation of Tie2 and CD31 in the mouse vascular endothelium using PEGylated cationic lipoplexes and targeted siRNA. The presence of PEG was observed to reduce toxicity *in vivo* as compared to nonPEGylated lipoplexes.[27] Lipoplexes were prepared by mixing pre-made PEGylated liposomes with siRNA such that the concentration of PEGylated lipids was 1%. An increase in the amount of PEG up to 5% resulted in the complete abolishment of gene silencing. In our study, we used 1.25 mol % of PEGylated lipids in the DDP formulation for cell and *in vivo* studies, and also observed that this concentration of PEG did not alter the specific downregulation of COX-2. We found that siRNA molecules delivered by DD or DDP cationic liposomes

specifically silenced COX-2 expression in cells. Our results also show that direct loading of siRNA did not influence the potency and specificity of siRNA-mediated silencing of cells in culture.

Incorporation of Gd-BOA contrast agents in DD or DDP liposomes resulted in nonspecific downregulation of protein expression in cultured cells. Transfection of MDA-MB-231 cells with liposomes for 24 h did not result in significant changes in cell viability. Transfection with directly loaded DD-COX-2 lipoplexes resulted in a small but statistically significant effect on the viability of MDAMB-231 cells. PEGylation of DD liposomes reversed the moderate toxicity of DD-COX-2 lipoplexes on cell viability with little, if any, effect on the potency and no effect on the specificity of the lipoplexes. These data are in agreement with previous data[15,28] where no cytotoxic effect was observed with DOTAP/DOPE liposomes.

To investigate the effects of the incorporation of iron-based contrast agents, we loaded DD liposomes with Feridex and corresponding siRNA complexes. Our results showed that Feridex incorporation into DD-COX-2 lipoplexes did not significantly affect their specificity. These data are consistent with the current use of Feridex as an intracellular contrast agent for cell tracking by MRI.[29]

To optically image the localization of DDP-delivered COX-2 siRNA *in vivo*, a DY647 moiety was covalently linked to the siRNA. Fluorescence was detected in tumor sections as early as 0.5 h after i.v. injection. The intracellular localization of DY647-labeled siRNA was observed, although more diffused, in the tumor tissue even 24 h post-injection despite the absence of specific tumor targeting moieties. The delivery of siRNA to the tumor cells through the leaky tumor vasculature is consistent with the enhanced permeability and retention effect observed with non-targeted liposome delivery.[30] Our data show that siRNA was delivered to the tumor most likely through the liposomes, and that the fluorescent signal at a later time point may arise from DY647-labeled DDP-COX-2 lipoplexes in the circulation. It is also possible that following COX-2 siRNA binding to endogenous COX-2 mRNA and its degradation by the RISC complex, free DY647 may have remained inside tumor cells.

The results of fluorescence microscopy of different organs indicate that a high fraction of DY647-labeled DDPFe-COX-2 siRNA lipoplex was found in the lungs, liver and spleen at earlier time points. These data are in agreement with previously published data on biodistribution of cationic liposome/oligonucleotide complex following intravenous injection.[31] In that study, the authors observed accumulation of cationic liposomes primarily in the liver and spleen and cationic liposomes/oligonucleotide complex in lungs at 15 min post i.v. injection that gradually redistributed to the liver by 24 h. In a different study, the influence of different serum components such as bovine serum albumin, lipoproteins (high-density lipoprotein and low-density lipoprotein) and macroglobulin on the delivery of cationic lipid/oligonucleotide complexes *in vivo* and in vitro was studied.[32] It was shown that oleic acid and heparin, found in the serum, would most likely affect the delivery *in vivo* and in vitro by displacing the oligonucleotide from the lipid complex. It was therefore suggested that incorporation of helper lipids such as cholesterol or DOPE would result in the delivery of the complex in the presence of serum in the medium. In the current study, we used DOPE as a helper lipid to reduce the interaction of the complex with serum in plasma.

We also demonstrated the ability to image the intratumoral delivery of COX-2 lipoplexes *in vivo* using MRI. DDPFe-COX-2 siRNA lipoplexes were detected in the tumor at 3 and 24 h post-injection using MR, and the presence of Feridex was confirmed by immunohisto-chemistry. AST and ALT levels in the serum of mice injected with DDPFe-COX-2 complex

were comparable to values obtained from uninjected control mice, indicating that the DDPFe-COX-2 lipoplexes did not induce liver toxicity.

Our findings demonstrate that metastatic MDA-MB-231 breast cancer cells can be efficiently transfected using COX-2 siRNA complexed with DD or DDP liposomes. COX-2 siRNA can be directly loaded into cationic DD and DDP liposomes without changing the siRNA functionality. The incorporation of MR contrast agents within liposomes creates the possibility of imaging siRNA delivery *in vivo* with MRI with a clear path of clinical translatability. In the future, MRI can be used to understand the effect of COX-2 siRNA delivery and downregulation on vascular and metabolic function.

Supplementary Material

Refer to Web version on PubMed Central for supplementary material.

Acknowledgments

This study was supported by NIH grants 2R01 CA 82337, NIH P50 CA103175, NIH U54 CA091409 (in collaboration with Dr Paul Wang at Howard University) and DOD-COE W81XWH-04-1-0595. We thank Drs Jan Hoh and Paul Wang for valuable scientific discussion, Mr Reza Hosseini for technical assistance and Mr Gary Cromwell for technical assistance with the animal studies.

References

1. Wang D, DuBois RN. Inflammatory mediators and nuclear receptor signaling in colorectal cancer. Cell Cycle 2007;6:682–685. [PubMed: 17374999]
2. De Marzo AM, Platz EA, Sutcliffe S, Xu J, Grönberg H, Drake CG, et al. Inflammation in prostate carcinogenesis. Nat Rev Cancer 2007;7:256–269. [PubMed: 17384581]
3. Diaz-Cruz ES, Brueggemeier RW. Interrelationships between cyclooxygenases and aromatase: unraveling the relevance of cyclooxygenase inhibitors in breast cancer. Anticancer Agents Med Chem 2006;6:221–232. [PubMed: 16712450]
4. Stasinopoulos I, O'Brien DR, Wildes F, Glunde K, Bhujwalla ZM. Silencing of cyclooxygenase-2 inhibits metastasis and delays tumor onset of poorly differentiated metastatic breast cancer cells. Mol Cancer Res 2007;5:435–442. [PubMed: 17510310]
5. Lasic DD. Colloid chemistry. Liposomes within liposomes. Nature 1997;387:26–27. [PubMed: 9139818]
6. Zelphati O, Szoka FC Jr. Intracellular distribution and mechanism of delivery of oligonucleotides mediated by cationic lipids. Pharm Res 1996;13:1367–1372. [PubMed: 8893276]
7. Xu L, Huang CC, Huang W, Tang WH, Rait A, Yin YZ, et al. Systemic tumor-targeted gene delivery by anti-transferrin receptor scFv-immunoliposomes. Mol Cancer Ther 2002;1:337–346. [PubMed: 12489850]
8. Sioud M, Sorensen DR. Systemic delivery of synthetic siRNAs. Methods Mol Biol 2004;252:515–522. [PubMed: 15017077]
9. Cardoso AL, Simoes S, de Almeida LP, Pelisek J, Culmsee C, Wagner E, et al. siRNA delivery by a transferrin-associated lipid-based vector: a non-viral strategy to mediate gene silencing. J Gene Med 2007;9:170–183. [PubMed: 17351968]
10. Foged C, Nielsen HM, Frokjaer S. Liposomes for phospholipase A2 triggered siRNA release: preparation and in vitro test. Int J Pharm 2007;331:160–166. [PubMed: 17156952]
11. Xia H, Mao Q, Paulson HL, Davidson BL. siRNA-mediated gene silencing *in vitro* and *in vivo*. Nat Biotechnol 2002;20:1006–1010. [PubMed: 12244328]
12. Ulrich AS. Biophysical aspects of using liposomes as delivery vehicles. Biosci Rep 2002;22:129–150. [PubMed: 12428898]
13. Sioud M, Sorensen DR. Cationic liposome-mediated delivery of siRNAs in adult mice. Biochem Biophys Res Commun 2003;312:1220–1225. [PubMed: 14652004]

14. Sorensen DR, Leirdal M, Sioud M. Gene silencing by systemic delivery of synthetic siRNAs in adult mice. J Mol Biol 2003;327:761–766. [PubMed: 12654261]
15. Pirollo KF, Zon G, Rait A, Zhou Q, Yu W, Hogrefe R, et al. Tumor-targeting nanoimmunoliposome complex for short interfering RNA delivery. Hum Gene Ther 2006;17:117–124. [PubMed: 16409130]
16. Pirollo KF, Rait A, Zhou Q, Hwang SH, Dagata JA, Zon G, et al. Materializing the potential of small interfering RNA via a tumor-targeting nanodelivery system. Cancer Res 2007;67:2938–2943. [PubMed: 17409398]
17. Hogrefe RI, Lebedev AV, Zon G, Pirollo KF, Rait A, Zhou Q, et al. Chemically modified short interfering hybrids (siHYBRIDS): nanoimmunoliposome delivery *in vitro* and *in vivo* for RNAi of HER-2. Nucleosides Nucleotides Nucleic Acids 2006;25:889–907. [PubMed: 16901821]
18. Sato A, Takagi M, Shimamoto A, Kawakami S, Hashida M. Small interfering RNA delivery to the liver by intravenous administration of galactosylated cationic liposomes in mice. Biomaterials 2007;28:1434–1442. [PubMed: 17141864]
19. Yano J, Hirabayashi K, Nakagawa S, Yamaguchi T, Nogawa M, Kashimori I, et al. Antitumor activity of small interfering RNA/cationic liposome complex in mouse models of cancer. Clin Cancer Res 2004;10:7721–7726. [PubMed: 15570006]
20. Bisanz K, Yu J, Edlund M, Spohn B, Hung MC, Chung LW, et al. Targeting ECM-integrin interaction with liposome-encapsulated small interfering RNAs inhibits the growth of human prostate cancer in a bone xenograft imaging model. Mol Ther 2005;12:634–643. [PubMed: 16039164]
21. Medarova Z, Pham W, Farrar C, Petkova V, Moore A. *In vivo* imaging of siRNA delivery and silencing in tumors. Nat Med 2007;13:372–377. [PubMed: 17322898]
22. Cailleau R, Young R, Olive M, Reeves WJ Jr. Breast tumor cell lines from pleural effusions. J Natl Cancer Inst 1974;53:661–674. [PubMed: 4412247]
23. Dass CR, Walker TL, Burton MA. Liposomes containing cationic dimethyl dioctadecyl ammonium bromide: formulation, quality control, and lipofection efficiency. Drug Deliv 2002;9:11–18. [PubMed: 11839204]
24. Fesus L, Thomazy V, Falus A. Induction and activation of tissue transglutaminase during programmed cell death. FEBS Lett 1987;224:104–108. [PubMed: 2890537]
25. Grosch S, Maier TJ, Schiffmann S, Geisslinger G. Cyclooxygenase-2 (COX-2)-independent anticarcinogenic effects of selective COX-2 inhibitors. J Natl Cancer Inst 2006;98:736–747. [PubMed: 16757698]
26. Li SD, Huang L. Targeted delivery of antisense oligodeoxynucleotide and small interference RNA into lung cancer cells. Mol Pharm 2006;3:579–588. [PubMed: 17009857]
27. Santel A, Aleku M, Keil O, Endruschat J, Esche V, Fisch G, et al. A novel siRNA-lipoplex technology for RNA interference in the mouse vascular endothelium. Gene Therapy 2006;13:1222–1234. [PubMed: 16625243]
28. Yu W, Pirollo KF, Rait A, Yu B, Xiang LM, Huang WQ, et al. A sterically stabilized immunolipoplex for systemic administration of a therapeutic gene. Gene Therapy 2004;11:1434–1440. [PubMed: 15229629]
29. Frank JA, Zywicke H, Jordan EK, Mitchell J, Lewis BK, Miller B, et al. Magnetic intracellular labeling of mammalian cells by combining (FDA-approved) superparamagnetic iron oxide MR contrast agents and commonly used transfection agents. Acad Radiol 2002;9(Suppl. 2):S484–S487. [PubMed: 12188316]
30. Matsumura Y, Maeda H. A new concept for macromolecular therapeutics in cancer chemotherapy: mechanism of tumoritropic accumulation of proteins and the antitumor agent smancs. Cancer Res 1986;46(12 Part 1):6387–6392. [PubMed: 2946403]
31. Litzinger DC, Brown JM, Wala I, Kaufman SA, Van GY, Farrell CL, et al. Fate of cationic liposomes and their complex with oligonucleotide *in vivo*. Biochim Biophys Acta 1996;1281:139–149. [PubMed: 8664312]
32. Zelphati O, Uyechi LS, Barron LG, Szoka FC Jr. Effect of serum components on the physico-chemical properties of cationic lipid/oligonucleotide complexes and on their interactions with cells. Biochim Biophys Acta 1998;1390:119–133. [PubMed: 9507083]

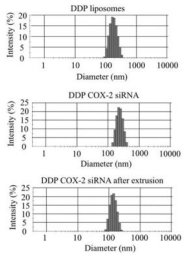

Figure 1.
Size distribution of DDPFe liposomes, cyclooxygenase-2 (COX-2) lipoplexes and lipoplexes after extrusion.

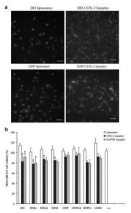

Figure 2.
Representative fluorescent images of (**a**) DD and DDP liposomes (left images) and internalization of DD and DDP-FITC (fluorescein 5(6)-isothiocyanate)-labeled cyclooxygenase-2 (COX-2) siRNA lipoplexes (right images) transfected in MDA-MB-231 breast cancer cells. Nuclei are labeled with DAPI (4,6-diamidino-2-phenylindole) (blue), bar 20 μm (**b**) MDA-MB-231 cell viability 24 h after incubation with liposomes, COX-2 and GAPDH lipoplexes.

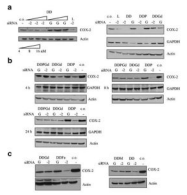

Figure 3.

(**a**, left panel) Immunoblotting analysis for cyclooxygenase-2 (COX-2) proteins in MDA-MB-231 breast cancer cells transfected with DD-COX-2 lipoplexes using different concentrations of siRNA. c.o.: cells only; L: Lipofectamine 2000; −2: COX-2 siRNA (100 nM). (**a**, right panel) Immunoblotting analysis of COX-2, GAPDH and actin proteins in MDA-MB-231 breast cancer cells transfected with DD, DDP and DDGd lipoplexes with COX-2 (−2) or GAPDH (−G) siRNA (40 nM). (**b**) Western blot analysis of COX-2, GAPDH and actin proteins in MDA-MB-231 breast cancer cells transfected with DDP, DDGd, DDPGd lipoplexes with COX-2 (−2) or GAPDH (−G) siRNA (40 nM) for 4, 8 and 24 h. (**c**) Western blot analysis of COX-2 and actin proteins from MDA-MB-231 breast cancer cells transfected with DD, DDGd, DDFe and DDM complexed with COX-2 (−2) or GAPDH (−G) siRNA (40 nM) siRNA lipoplexes.

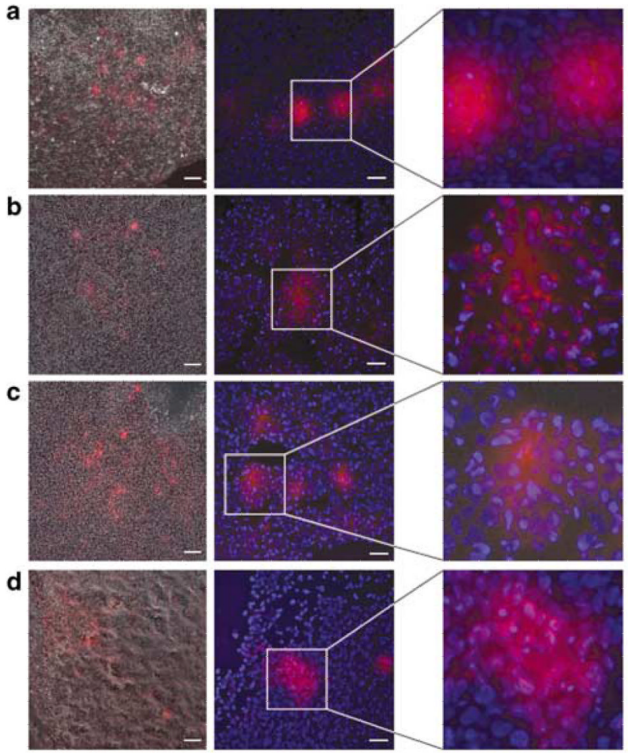

Figure 4.
DY647-labeled cyclooxygenase-2 (COX-2) DDP lipoplexes localization in fresh tumor sections (**a**) 0.5 h (*n* = 4), (**b**) 3h (*n* = 3), (**c**) 8h (*n* = 3) and (**d**) 24h (*n* = 3) post-injection. Left panel represents phase-contrast images overlayed with fluorescence images. Left column: × 10 objective, bar 50 μm; middle column: × 40 objective, bar, 20 μm and right column: pixel-level magnification. Images were acquired using a Cy5.5 filter, and an exposure time of 2 s.

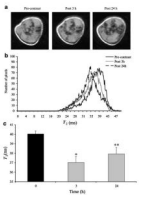

Figure 5.

(**a**) Representative T_2-weighted images of tumors from mice injected with DDPFe-COX-2 (cyclooxygenase-2) lipoplexes (n = 5) obtained at 3 and 24 h post-injection; images were obtained with a spatial resolution of 0.125 mm × 0.125 mm × 0.125 mm. (**b**) Histograms were computed from T_2 maps and demonstrated a major shift in T_2 values at 3 and 24 h and (**c**) quantitative analysis of T_2 maps demonstrating a significant decrease of T_2 values at 3 h (*P<0.004, n = 5) and 24 h (**P = 0.02, n = 5).

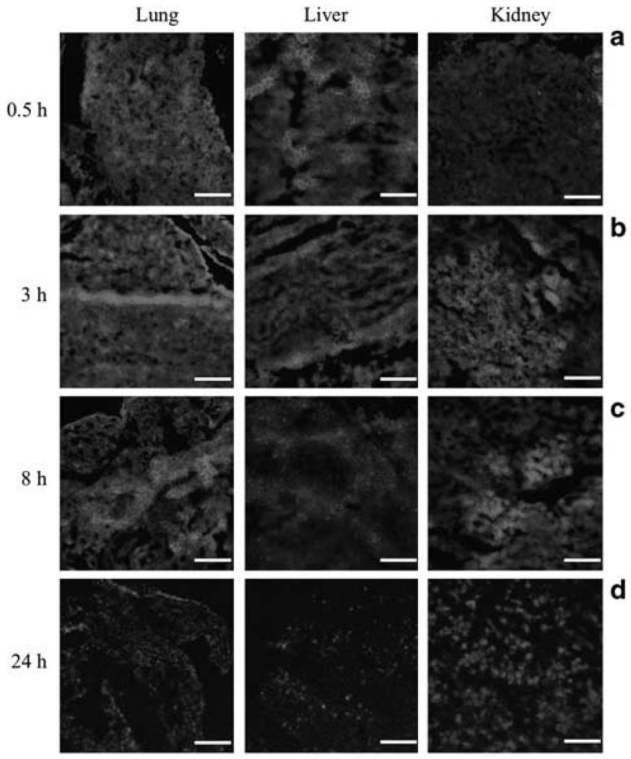

Figure 6.
Fluorescence microscopy images of lung, liver and kidney sections at 0.5 h (**a**), 3 h (**b**), 8 h (**c**) and 24 h (**d**) after i.v. administration of DY647-labeled COX-2 DDP lipoplexes in mice, bar 20 μm. Images were acquired using a Cy5.5 filter and identical exposure times.

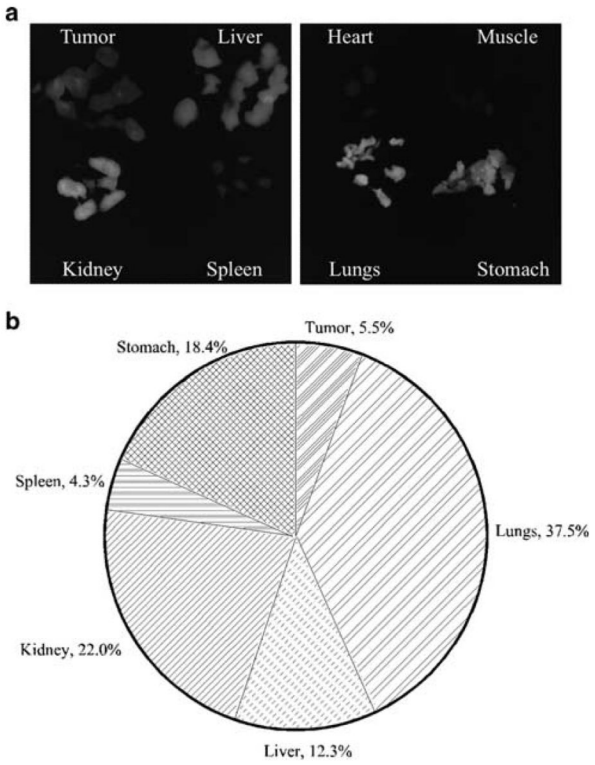

Figure 7.

(**a**) Fluorescence images of 1-mm-thick slices of tumor and organs of mice injected with DY647-labeled COX-2 DDP lipoplexes (n = 3) at 24 h post i.v. injection. Images were acquired using Cy5.5 filter, at f/4, 1 s. (**b**) Quantitative analysis of fluorescence images from tumor and organ slices at 24 h post-injection. The pie chart represents 100% of detectable fluorescence at 24 h post-injection.

Table 1

Hydrodynamic diameter (*d*, nm), polydispersity index (PDI) and ζ potential for COX-2 DD and DDP lipoplexes

COX-2 lipoplex	Diameter (nm)	Polydispersity index	ζ potential (mV)
DD	289 ± 10	0.172 ± 0.012	43.6 ± 3.4
DDFe	304 ± 13	0.272 ± 0.030	31.3 ± 3.5
DDGd	265 ± 10	0.396 ± 0.030	31.4 ± 1.4
DDM	291 ± 24	0.238 ± 0.018	44.0 ± 2.5
DDP	183 ± 16	0.200 ± 0.033	28.0 ± 0.1
DDPFe	277 ± 19	0.200 ± 0.020	30.0 ± 1.5
DDPGd	162 ± 13	0.197 ± 0.046	17.2 ± 15

Abbreviation: COX-2, cyclooxygenase-2.